Torque Ripple Reduction Design Approach of Permanent Magnet Machines Based on Circumferential Pole Pair Shift

Litao Dai[1], Shuangxia Niu[1], Jian Gao[2], and Shoudao Huang[2]

[1]Department of Electrical and Electronic Engineering, The Hong Kong Polytechnic University, Hong Kong, 999077, China
[2]College of Electrical and Information Engineering, Hunan University, Changsha, 410002, China

To tackle the torque pulsation challenge in permanent magnet machines, this paper proposes two design methods that involve shifting the permanent magnet pole-pairs. Method 1 circumferentially shifts half of the pole-pairs by half of the most significant pulsation period, while Method 2 shifts multiple pole pairs, with the angle of pole-pair displacement gradually increasing and evenly distributed over one selected pulsation cycle. Through finite element method of various case studies with diverse pole-slot combinations, it is demonstrated that both proposed methods effectively suppress torque ripple, reduce cogging torque, and optimize back-electromotive force distortion.

***Index Terms*—Permanent magnet machines, permanent magnet motors, torque, design optimization.**

I. Introduction

PERMANENT MAGNET machines (PMMs) are extensively used in industrial applications due to their significant advantages of high torque density and efficiency. Nonetheless, a notable drawback of PMMs is their tendency for torque ripple issues, which can impair control performance and contribute to shaft fatigue [1]. Therefore, minimizing torque ripple is crucial for the high-end applications of PMMs [2].

Various factors contribute to the torque ripple of PMMs, including cogging torque, synchronous torque ripple, reluctance torque ripple, and current harmonic-induced torque ripple. To achieve low torque ripple operation of motor applications, two main approaches can be employed. The first involves designing a motor with inherently low torque ripple and further controlled by sinusoidal current excitation [3]. The second approach involves injecting current harmonics during operation to suppress torque ripple [4]. In comparison, the second approach is more complex and often compromises motor dynamic performance due to the required regulation of harmonic currents. Therefore, optimizing motor design using the first way to reduce torque ripple is generally preferred [5].

Various effective methods have been proposed for the design optimization of torque ripple, generally classified into three categories: 1) PM flux optimization, 2) winding magnetomotive force (MMF) optimization, and 3) reluctance optimization.

Firstly, the PM flux optimization method involves structuring the motor side that contains the PM and generates magnetic flux. Optimization techniques in this realm include altering the PM shape [6], modifying the structure of multiple PM layers [7], [8], adjusting the rotor flux barrier [9], fine-tuning the rotor core surface profile [3], and incorporating asymmetric rotor poles, [10]. Through the optimization of these structures, the flux harmonics contributing to torque ripple can be adjusted to reduce overall ripple effects.

Secondly, winding MMF optimization involves adjusting the winding arrangement to optimize MMF harmonics for reducing torque ripple. To achieve this, a wye-delta winding structure is proposed to minimize interactive harmonics in fractional-slot PMMs [11]. Additionally, a phase winding module and tooth shoes shift method have been introduced to enhance fault-tolerant capability while reducing torque ripple [12].

Lastly, the reluctance optimization method is achieved through design the motor structure that exhibits uneven magnetic reluctance characteristics, such as stator and rotor teeth. By modifying reluctance structures, the reluctance harmonics can be adjusted to reduce torque ripple [13], with a significant impact on cogging torque in particular [14], [15].

The aforementioned methods are effective in reducing torque ripple. However, they may lead to certain undesired effects, such as decreased average torque [6], [12], [13], [14], [15], increased optimization challenges [7], [8], [9], [16], reduced mechanical robustness [10], increased manufacturing complexities [11], and so on.

Hence, it is valuable to explore an efficient torque ripple reduction method that is easy to implement, minimally compromises critical electromagnetic performances, doesn't add manufacturing difficulties or costs.

In this context, this paper introduces a novel pole-pair circumferential shifting method. This method has minimal undesirable effects while effectively reducing torque ripple. To validate its effectiveness and broad applicability, diverse motor case studies are conducted, covering various pole-slot combinations.

The article is structured as follows: Section II presents the torque ripple model. Section III elaborates on the proposed method and its principles. Section IV conducts four case studies to confirm the effectiveness and versatility. Finally, Section V concludes the article.

II. Electromagnetic Torque and Its Pulsation

The electromagnetic torque comprises three torque components: cogging torque, synchronous torque, and reluctance torque. In the context of three-phase PMMs, as per the harmonic interaction model [3], these torques exhibit similar fluctuating patterns, specifically $6n$ times the electrical frequency (n=1, 2, …). The harmonic forms, sources of torque ripple, and their modes of existence are depicted in Fig. 1. In summary, irrespective of the intricate ripple sources, the ultimate torque ripple conforms to the $6n$ pattern.

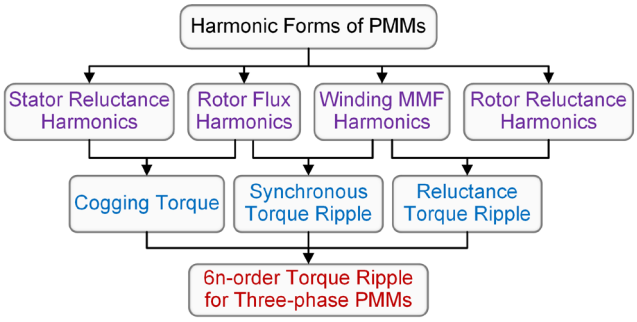

Fig. 1. Overview of harmonic forms and torque ripple components in PMMs.

Hence, the torque can be decomposed into dc and ac components, expressed as follows

$$T_{\mathrm{EM}} = T_{\mathrm{EM0}} + T_{\mathrm{EM1}} \tag{1}$$

where T_{EM0} is the dc component, which is constant and can be utilized for energy conversion, while T_{EM1} is the ac component, characterized by undesirable pulsating form that should be minimized to zero.

Furthermore, the torque pulsation component can be expressed uniformly as the following Fourier series

$$T_{\mathrm{EM1}} = \sum_{n=1,2,\ldots} A_{\mathrm{TE}}(n)\cos(6np_N\omega_m t + \varphi_{\mathrm{TE}}(n)) \tag{2}$$

where p_N, ω_m, and t denote the pole-pair number, mechanical speed, and operating time, respectively. A_{TE}, φ_{TE} are the amplitude and phase of torque ripple, which are related to the torque ripple order n.

From another point of view, for motors with multiple pole-pairs, the torque pulsation can always be considered as a result of superposition of multiple pole-pair units of the motor, since the motor is periodically symmetrical.

For better demonstration, a schematic decomposition of the electromagnetic torque of a motor with 4 pole-pairs (integer-slot) is shown in Fig. 2. As seen from the diagram the torque pulsation can be decomposed into both $6n$ times the pulsation component by Fourier transformation, but also into a combination of different pole-pairs with the same amplitude.

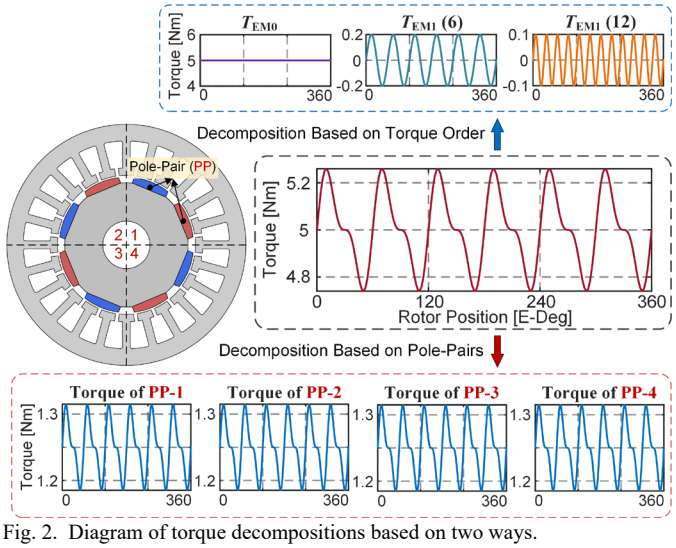

Fig. 2. Diagram of torque decompositions based on two ways.

III. Principle of the Proposed Methods

In this section, a comprehensive design approach for reducing torque ripple through pole-pair circumferential shifting is introduced. The discussion covers two shifting methods, each offering a distinct perspective. Variations in the form and angle of pole-pair shifting between the methods lead to differences in the targeted order of torque ripple.

A. Proposed Method I: Pole-Pair Reverse Shifting

Method 1 involves shifting half of the motor pole-pairs by an angle equivalent to half of the most significant torque pulsation period. This approach theoretically aims to eliminate the most significant order of torque pulsation.

Fig. 3 illustrates a schematic representation of the proposed reverse shifting method (RSM), where the 2nd and 4th pole-pairs are shifted. The calculation for the shifting angle is determined as follows

$$\text{RSM:}\quad \theta_{s1} = \frac{1}{2}\theta_{TM}, \qquad \theta_{TM} = \frac{360}{6n_M p_N} \tag{3}$$

where θ_{TM} denotes the circumferential angle corresponding to the most significant torque pulsation order n_M.

B. Proposed Method II: Pole-Pair Gradual Shifting

In Method 2, each pole-pair of the motor undergoes a unique angle shift, with the shifted angles progressively increasing to form a torque pulsation cycle. This method is theoretically capable of reducing multiple orders of torque pulsation.

The schematic diagram of the proposed gradual shifting method (GSM) is depicted in Fig. 4. The calculation for the shifting angles of different pole-pairs is as follows:

$$\text{GSM:}\quad \theta_{s2} = \frac{k_{pN}}{p_N}\theta_{TB}\,, \qquad k_{pN} = 1, 2, \ldots, (p_N - 1) \tag{4}$$

where θ_{TB} represents the basic torque pulsation period, which is particularly effective when the torque ripple order is low.

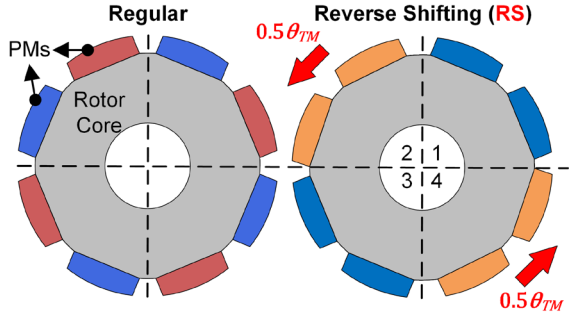

Fig. 3. Illustration of the proposed RSM.

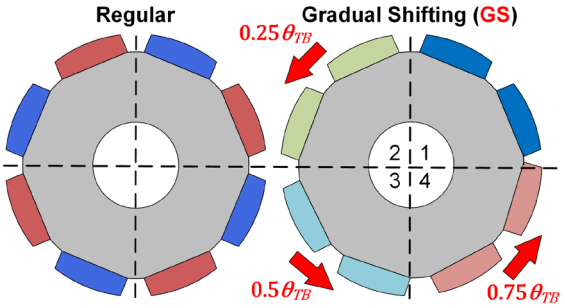

Fig. 4. Illustration of the proposed GSM.

C. Demonstration of Torque Ripple Reduction Principle

In the presented methods, the torque waveforms for different pole pairs and the synthesized torque are illustrated in Fig. 5. It is seen that the RSM effectively mitigates the most prominent order of torque ripple ($6th$), whereas the GSM reduces multiple orders of torque ripple ($6th$ and $12th$).

The underlying principle of these two methods for eliminating torque ripple involves offsetting the pole pairs such that the maximum and minimum values of torque pulsation generated by different pole pairs overlap and cancel each other out. Notably, the GSM's ability to suppress multiple torque ripple orders can be attributed to its more refined shifting angles, which enable higher torque harmonics to be counteracted.

Furthermore, the total harmonic distortion (THD) of back-EMF also benefits from pole-pair shifting, as the EMF harmonics are similarly counteracted, particularly when their orders are close to those of the torque ripple.

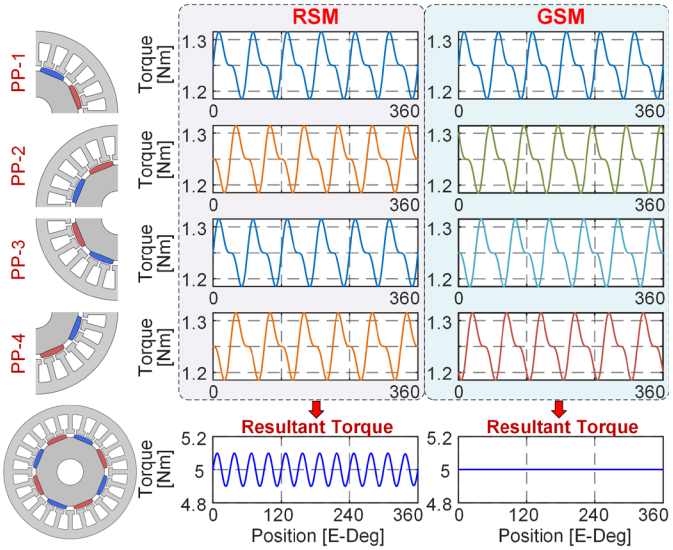

Fig. 5. Principle diagram of the proposed methods on torque ripple reduction.

IV. Case Studies

To validate the effectiveness of the proposed methods, four motor cases involving various pole-slot combinations, encompassing integer and fractional slots, as well as concentrated and distributed configurations, are analyzed and confirmed using the finite element method (FEM).

All case studies adhere to uniform structure parameters, as outlined in Table I, featuring the surface-mounted rotor with bread-type PMs.

TABLE I
Uniform Structural Parameters of Case Studies

Parameter	Value	Parameter	Value
Motor diameter (mm)	150	Ratio of stator bore	0.6
Motor length (mm)	60	Ratio of tooth width	0.5
Airgap thickness (mm)	1	Ratio of slot opening	0.4
Slot fill factor (Copper)	0.4	Ratio of slot depth	0.65
Current density, rms (A/mm^2)	3	Ratio of pole arc	0.7

A. Case I: 8-Pole 12-Slot PMM

In this pole-slot configuration, both the torque ripple and cogging torque fundamental frequencies are six times the electrical frequency, allowing the determination of the shifting angles for the two methods. The initial motor design and the motor utilizing these two methods underwent simulation and comparison, showcasing the motor's magnetic flux lines and densities, electromagnetic torque, cogging torque, phase back electromotive force (EMF), and their fast-Fourier transform (FFT) comparisons in Fig. 6.

Table 2 offers a comprehensive performance evaluation of the three approaches. It is evident that there are significant enhancements in torque ripple, cogging torque, and back EMF distortion.

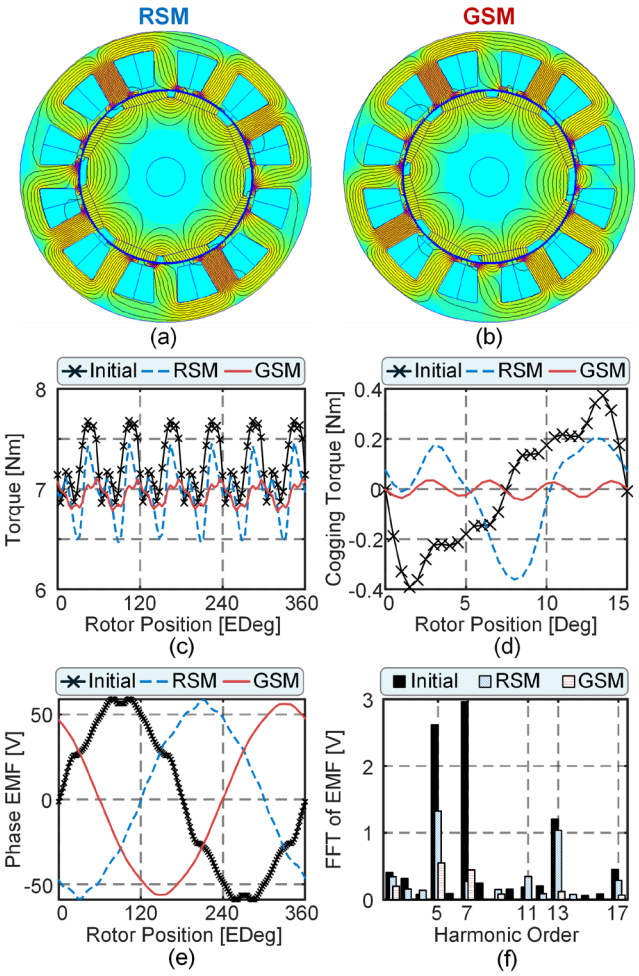

Fig. 6. Comparison results of Case I. (a) Motor with RSM. (b) Motor with GSM. (c) Electromagnetic torque. (d) Cogging Torque. (e) Phase back-EMF (f) FFT of the EMF.

TABLE II
Electromagnetic Performance Comparison of Case-I

Characteristics	Regular	RSM	GSM
Shifting angle (MDeg)	/	$\theta_{TM} = 15$	$\theta_{TB} = 15$
Torque ripple (%)	11.34	14.34	4.67
Cogging torque, peak-peak (Nm)	0.76	0.57	0.08
THD of phase back-emf (%)	7.26	3.2	1.31

B. Case II: 8-Pole 24-Slot PMM

The fundamental frequencies of the torque ripple and cogging torque coordinated with this pole-slot configuration are both six times the electrical frequency, resulting in the periodic shifting angles for the two methods remaining at 15 degrees.

Based on this, three motor structures were subjected to simulation analysis, with the motor field plot and waveforms of torque, cogging torque, and phase back-EMF shown in Fig. 7, and a comparison of electromagnetic performance presented in Table III. Comparing these results reveals that the two proposed methods offer varying degrees of optimization for torque ripple, cogging torque, and back EMF harmonic distortion.

TABLE III
ELECTROMAGNETIC PERFORMANCE COMPARISON OF CASE-II

Characteristics	Regular	RSM	GSM
Shifting angle (MDeg)	/	$\theta_{TM} = 15$	$\theta_{TB} = 15$
Torque ripple (%)	20.28	15.27	8.2
Cogging torque, peak-peak (Nm)	0.77	0.81	0.17
THD of phase back-emf (%)	17.21	8.91	7.24

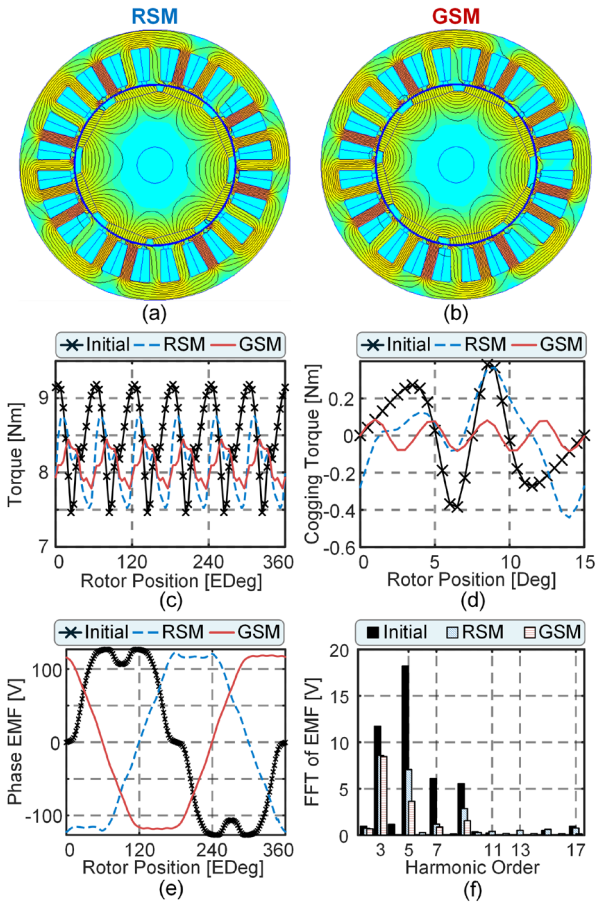

Fig. 7. Comparison results of Case II. (a) Motor with RSM. (b) Motor with GSM. (c) Torque. (d) Cogging Torque. (e) Phase EMF. (f) FFT of the EMF.

C. Case III: 8-Pole 48-Slot PMM

This integer-slot distributed-winding motor configuration is a classic solution for electric vehicles, with its torque ripple and cogging torque fundamental frequencies being six times and twelve times the electrical frequency, respectively. In this study, the angle period for the two shifting schemes is uniformly set at 7.5 degrees. Based on this, the simulation results for the three schemes are illustrated in Fig. 8, with the performance comparison detailed in Table IV. A comparison of these results reveals a very noticeable suppression of torque ripple, particularly significant suppression of cogging torque.

TABLE IV
ELECTROMAGNETIC PERFORMANCE COMPARISON OF CASE-III

Characteristics	Regular	RSM	GSM
Shifting angle (MDeg)	/	$\theta_{TM} = 7.5$	$\theta_{TB} = 7.5$
Torque ripple (%)	15.2	10.18	6.42
Cogging torque, peak-peak (Nm)	0.68	0.45	0.02
THD of phase back-emf (%)	9.35	7.56	7.02

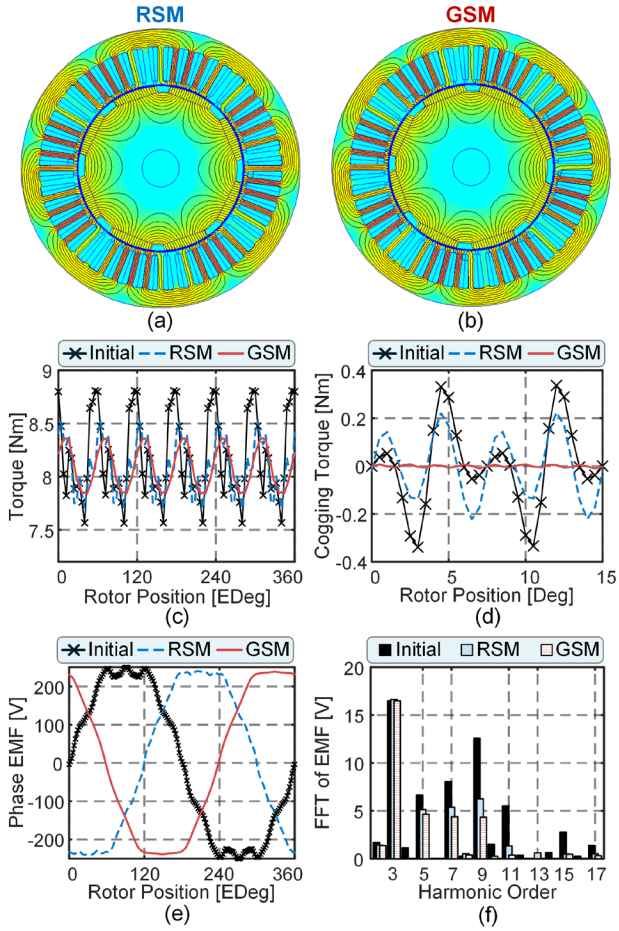

Fig. 8. Comparison results of Case III. (a) Motor with RSM. (b) Motor with GSM. (c) Torque. (d) Cogging Torque. (e) Phase EMF. (f) FFT of the EMF.

D. Case IV: 20-Pole 24-Slot PMM

This case represents a classic fractional-slot concentrated winding motor scheme. RSM was employed in this scenario. Simulation comparisons are shown in Fig. 9, while performance evaluations are elaborated in Table V.

Notably, GSM was omitted in this instance due to the necessity for pole-pair adjustments to conform to the three-phase symmetry principle. According to theory, a magnetic pole offset plan should encompass at least one motor unit, yet in this case, the 10-pole 12-slot layout constitutes a singular motor unit. Hence, RSM was the only permissible method in this context.

It is evident that even though the initial design exhibited excellent torque performance, further optimizations could still be achieved through RSM-based design.

TABLE V
ELECTROMAGNETIC PERFORMANCE COMPARISON OF CASE-IV

Characteristics	Regular	RSM
Shifting angle (MDeg)	/	$\theta_{TM} = 3$
Torque ripple (%)	1.85	0.41
Cogging torque, peak-peak (Nm)	0.126	0.0197
THD of phase back-emf (%)	1.33	1.55

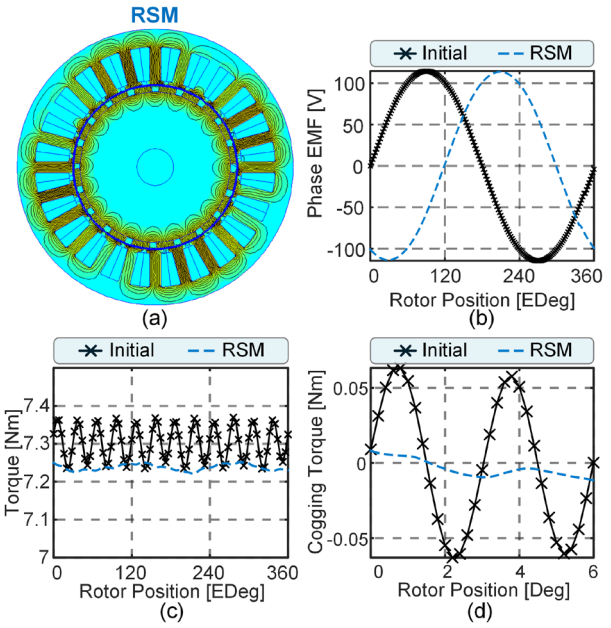

Fig. 9. Comparison results of Case IV. (a) Motor with RSM. (b) Phase EMF. (c) Torque. (d) Cogging Torque.

V. CONCLUSION

This study investigates the circumferential shifting technique of the rotor magnetic field in PMMs to alleviate torque ripples, introducing the pole-pair shifting methods of RSM and GSM. Through rigorous case studies involving diverse pole-slot configurations, the following conclusions are derived:

1. All case studies validate the effectiveness of the proposed methods in mitigating torque ripple, reducing cogging torque, and suppressing EMF distortion. Notably, these benefits are achieved without increasing manufacturing cost or complexity. Specifically, GSM shows superior performance compared to RSM, as its gradual shifting mechanism enables the counteraction of higher-order torque and EMF harmonics.
2. Although the presented cases focus on surface-mounted PM structures, the authors' investigations suggest that the proposed methods are equally applicable to interior PM machines without compromising motor efficiency. Furthermore, the underlying principle of these methods holds promise for adaptation to other PM machine topologies, such as linear machines and axial flux PM machines.
3. Regarding the limitations of the proposed methods, pole-pair shifting necessitates grounding within the entire motor unit to maintain winding balance. For instance, a 20-pole, 24-slot motor is constructed based on a 10-pole, 12-slot unit. Additionally, serious considerations should be given to the issues of flux-leakage and torque compromise arising from pole-pair shifting.

ACKNOWLEDGEMENT

This work was supported by the National Natural Science Foundation of China under Project 52077187

REFERENCES

[1] T. M. Jahns and W. L. Soong, "Pulsating torque minimization techniques for permanent magnet AC motor drives-a review," *IEEE Trans. Ind. Electron.*, vol. 43, no. 2, pp. 321-330, April 1996.

[2] M. S. Rafaq, W. Midgley and T. Steffen, "A Review of the State of the Art of Torque Ripple Minimization Techniques for Permanent Magnet Synchronous Motors," *IEEE Trans. Ind. Inform.*, vol. 20, no. 1, pp. 1019-1031, Jan. 2024.

[3] L. Dai, S. Niu, W. Zhang, J. Gao and S. Huang, "Harmonic Modeling and Ripple Suppression of Electromagnetic Torque in IPMSMs," *IEEE Trans. Ind. Electron.*, vol. 71, no. 12, pp. 16223-16233, Dec. 2024.

[4] G. Feng, C. Lai and N. C. Kar, "A Novel Current Injection-Based Online Parameter Estimation Method for PMSMs Considering Magnetic Saturation," *IEEE Trans. Magn.*, vol. 52, no. 7, pp. 1-4, July 2016, Art no. 8106004.

[5] D. G. Dorrell, M. -F. Hsieh, M. Popescu, L. Evans, D. A. Staton and V. Grout, "A Review of the Design Issues and Techniques for Radial-Flux Brushless Surface and Internal Rare-Earth Permanent-Magnet Motors," *IEEE Trans. Ind. Electron.*, vol. 58, no. 9, pp. 3741-3757, Sept. 2011.

[6] J. Qi et al., "Suppression of Torque Ripple for Consequent Pole PM Machine by Asymmetric Pole Shaping Method," *IEEE Trans. Ind. Appl.*, vol. 58, no. 3, pp. 3545-3557, May-June 2022.

[7] Y. Shimizu, S. Morimoto, M. Sanada and Y. Inoue, "Investigation of Rotor Topologies for Reducing Torque Ripple in Double-Layer IPMSMs for Automotive Applications," *IEEE Trans. Ind. Electron.*, vol. 70, no. 8, pp. 8276-8285, Aug. 2023.

[8] L. Dai, J. Gao, S. Niu and S. Huang, "Multi-Electromagnetic Performance Optimization of Double-Layer Interior Permanent Magnet Synchronous Machine," *IEEE Trans. Ind. Electron.*, vol. 71, no. 11, pp. 14535-14545, Nov. 2024.

[9] T. -A. Huynh, Y. -T. Nguyen Le, Z. Lee, M. -C. Tsai, P. -W. Huang and M. -F. Hsieh, "Influence of Flux Barriers and Permanent Magnet Arrangements on Performance of High-Speed Flux-Intensifying IPM Motor," *IEEE Trans. Magn.*, vol. 59, no. 11, pp. 1-6, Nov. 2023, Art no. 8203606.

[10] Q. Chen, J. Liao, Z. Sang, W. Qian, G. Xu and Z. Liu, "Design and Analysis of a Novel Hybrid Rotor PM Machine Considering Negative Torque Ripple Contribution," *IEEE Trans. Ind. Electron.*, vol. 71, no. 7, pp. 6775-6786, July 2024.

[11] M. S. Islam, R. Mikail, M. A. Kabir and I. Husain, "Torque Ripple and Radial Force Minimization of Fractional-Slot Permanent Magnet Machines Through Stator Harmonic Elimination," *IEEE Trans. Transport. Electrific.*, vol. 8, no. 1, pp. 1072-1084, March 2022.

[12] J. Li, W. Zhao, X. Zhao, J. Ji and Y. Sun, "Phase Winding Module Design of Fault-Tolerant Permanent-Magnet Machine With Reduced Torque Ripple," *IEEE Trans Energy Convers.*, vol. 39, no. 3, pp. 1804-1817, Sept. 2024.

[13] P. Wang, W. Hua, G. Zhang, B. Wang and M. Cheng, "Torque Ripple Suppression of Flux-Switching Permanent Magnet Machine Based on General Air-Gap Field Modulation Theory," *IEEE Trans. Ind. Electron.*, vol. 69, no. 12, pp. 12379-12389, Dec. 2022.

[14] Y. -J. Won, J. -H. Kim, S. -M. An and M. -S. Lim, "Comparative Study of Cogging Torque, Torque Ripple, and Vibration on Stator Tooth Chamfer Types in Permanent Magnet Synchronous Motors," *IEEE Trans. Magn.*, vol. 60, no. 9, pp. 1-5, Sept. 2024, Art no. 8202905.

[15] L. Dai, J. Gao, S. Niu, K. Liu, S. Huang and W. L. Chan, "Cogging Torque Suppression for IPMSM Based on Flux Harmonic Configuration," *IEEE Trans. Ind. Electron.*, Early Access, Doi: 10.1109/TIE.2024.3443959.

[16] Q. Lin, S. Niu, F. Cai, W. Fu and L. Shang, "Design and Optimization of a Novel Dual-PM Machine for Electric Vehicle Applications," *IEEE Trans. Veh. Technol.*, vol. 69, no. 12, pp. 14391-14400, Dec. 2020, doi: 10.1109/TVT.2020.3034573.